An *In Vitro* Nerve Agent Brain Poisoning Transwell Model for Convenient and Accurate Antidote and Nanomedicine Evaluation

Yao Li
Beijing Institute of Pharmacology and Toxicology: Academy of Military Medical Sciences Institute of Pharmacology and Toxicology

Jingyi Huang
Beijing Institute of Pharmacology and Toxicology: Academy of Military Medical Sciences Institute of Pharmacology and Toxicology

Huanchun Xing
Beijing Institute of Pharmacology and Toxicology: Academy of Military Medical Sciences Institute of Pharmacology and Toxicology

Zinan Zhang
Beijing Institute of Pharmacology and Toxicology: Academy of Military Medical Sciences Institute of Pharmacology and Toxicology

Xin Sui
Beijing Institute of Pharmacology and Toxicology: Academy of Military Medical Sciences Institute of Pharmacology and Toxicology

Yuan Luo
Beijing Institute of Pharmacology and Toxicology: Academy of Military Medical Sciences Institute of Pharmacology and Toxicology

Yongan Wang
Beijing Institute of Pharmacology and Toxicology: Academy of Military Medical Sciences Institute of Pharmacology and Toxicology

Jun Yang (ajaway@126.com)
Beijing Institute of Pharmacology and Toxicology: Academy of Military Medical Sciences Institute of Pharmacology and Toxicology https://orcid.org/0000-0002-4901-8530

Research

Keywords: Nerve agents, blood–brain barrier, central poisoning, therapeutic effect, nanomedicine

Posted Date: April 14th, 2021

DOI: https://doi.org/10.21203/rs.3.rs-418345/v1

Abstract

Background: Nerve agents (NAs) can irreversibly inhibit acetylcholinesterase (AChE). An effective NA antidote should permeate the blood–brain barrier (BBB) to reactivate the inhibited AChE in brain. There is an urgent requirement for the large-scale evaluation and screening of antidotes. Existing methods for evaluating reactivators *in vitro* can only examine the reactivation effect of drugs and not brain-target properties. The current Transwell BBB model can only evaluate the drug penetration performance for crossing the barrier, but not the pharmacodynamics.

Methods: Highly purified rat brain microvascular endothelial cells (RBMECs) from 2-week-old Sprague Dawley rats were inoculated into the upper chamber of Transwell plates to establish a BBB model. Three key parameters of AChE reactivation were determined by the Ellman method: the minimum detection limit of AChE, the effective dosage of NAs (70% enzyme inhibition rate), and the optimal dosage of reactivators. AChE and NAs were added to the lower pool of Transwell plates to simulate central poisoning, and antidotes of reactivators were added to the upper pool to simulate drug administration. The AChE activity of samples, collected from the lower pool, was measured. A liposomal nanomedicine loaded with the reactivator asoxime chloride (HI-6) was prepared using the extraction method and tested by the model.

Results: The obtained RBMECs exhibited a typical monolayer “paving stone” morphology, and tight junctions were expressed among the RBMECs. The concentrations of AChE, sarin, and the reactivator were 0.07 mg/mL, 10^{-6} v/v, and 0.03 mg/mL, respectively. The reaction rate of the reactivators obtained from the model was significantly lower than that obtained from the non-model group. Furthermore, a nanomedicine loaded with HI-6 was synthesized. The final results and rules obtained from the model were in accordance with those evaluated *in vivo*.

Conclusion: The therapeutic effect of antidotes can be rapidly and accurately evaluated using this model. In addition to small-molecule drugs, nanomedicines can also be evaluated by this method. A liposomal nanomedicine with a high reactivation rate against the nerve agent sarin was discovered.

Background

Nerve agents (NAs) are the most toxic synthetic chemicals known [1, 2]. Many countries are equipped with them, and they have been utilized in several instances of local warfare, such as in the Iraq–Iran War [3] and Syrian civil war [4, 5], leading to great casualties. In recent years, these chemicals have been used in terrorism attacks, such as the Tokyo subway sarin attack [6], and assassination attempts, such as the poisoning of Sergei and Yulia Skripal in Salisbury, England [7, 8] and the assassination of Kim Jong-nam in Malaysia [9]. NAs can rapidly and irreversibly inhibit AChE in the brain and prevent the hydrolysis of the neurotransmitter acetylcholine (ACh), leading to hyperfunction of the cholinergic system [10]. Without an effective antidote, exposure to NAs can cause immediate mortality [11]; thus, the synthesis and evaluation of an effective antidote is urgently needed.

Antidotes must satisfy two fundamental requirements for effective detoxification against NAs [12, 13]. First, they must cross the blood–brain barrier (BBB) and target the brain. Second, they must show good performance in attacking the toxic agent molecules and separating the agent from the AChE to reactivate hydrolysis. At present, a great number of synthesized candidate antidotes need to be evaluated for further research. For *in vitro* evaluation, these candidate antidotes are mixed with a certain dosage of NAs directly and AChE in tubes and measured by the date of activity of the enzyme AChE [14]. This *in vitro* evaluation method only considers the interaction between the antidote and NAs and the reactivation effect, but not the brain-targeting properties. Therefore, many of the candidate antidotes were effective *in vitro*, but invalid for animal detoxification in instances of real NA poisoning. The mature Transwell system of the BBB model inoculated with RBMECs in the membrane can successfully simulate the barrier function *in vitro* [15–17]. However, this model only reflects the ability of the drug to penetrate the barrier layer, but not the pharmacodynamics of detoxification.

The detoxification effect of the antidote is evaluated more generally *in vivo* [13, 18]. However, several inherent bottlenecks restrict the utilization of animal experiments in real NA poisoning and detoxification evaluations, such as the high dosage NA for animal poisoning, marked differences between animal individuals, large numbers of animals required for experimentation, complex and time-consuming experimental processes, and inaccurate results. Therefore, in the preliminary stage of drug screening, it is necessary to develop a method to evaluate brain-targeted detoxification by the candidate antidote with safety, rapidness, accuracy, convenience, using high-throughput screening.

In this study, a model based on the Transwell system was proposed to simulate brain poisoning for antidote evaluation (Fig. 1a-b). First, RBMECs were cultured and planted on the membrane of the Transwell system to construct a barrier effect. Then, the antidote, nerve agent, and AChE were added into different chambers of the Transwell system to simulate systemic administration to detoxify brain poisoning. Using this modified model, the reactivation rates of existing common reactivators were tested and compared with the data obtained from traditional *in vitro* and *in vivo* methods to verify the effectiveness, accuracy, and convenience of the model. Furthermore, a nano-reactivator was synthesized and evaluated using a modified model to determine the real detoxification effect in mice. The *in vitro* and *in vivo* results obtained were consistent, suggesting that the modified model could truly and successfully reflect the therapeutic effect of the candidate antidote against nerve agent brain poisoning.

Materials And Methods

Reagents

All reagents were purchased from Sigma-Aldrich (Darmstadt, GER) unless otherwise stated. Endothelial cell medium (ECM) was purchased from ScienCell (Carlsbad, CA, USA). Fetal bovine serum and phosphate-buffered saline (PBS) were purchased from Gibco (Waltham, MA, US). Bovine serum albumin was purchased from VWR (Monroeville, PA, USA). Cell Counting Kit-8 (CCK-8) was purchased from

Dojindo (Kumamoto, Japan). Dipalmitoylphosphatidylcholine (DPPC) was purchased from TCI (Tokyo, Japan).

RBMEC study

High activity RBMECs were isolated from 2-week-old Sprague Dawley rats by two-step enzyme digestion, density gradient centrifugation, and differential adhesion in sequence [18, 19]. The extracted primary cells were cultured in T25 culture flasks at a seeding density of 2×10^5 cells/mL, and the medium was changed every 2–3 days.

The growth curve and morphology of the cells were monitored by microscopy and CCK-8 assays daily after seeding in 96-well plates and T25 culture bottles at a density of 1×10^5 cells/mL. Six days later, the cells were collected by separating them from the bottle with a cell scraper and centrifuging for 5 min (1000 rpm, 25 ℃), fixed, dehydrated using 3% paraformaldehyde and alcohol, and observed via transmission electron microscopy (TEM).

Establishment And Characterization Of The Transwell System

The isolated RBMECs were planted on the membrane of the Transwell system at a seeding density of 2×10^5 cells/mL [20]. The growth curve of the cell barrier layer was monitored daily via the transendothelial electrical resistance (TEER) assay using an epithelial volt/ohm meter (Millicell® ERS-2; Millipore, Bedford, MA, USA). The effective resistance was calculated using the following formula:

Effective resistance ($\Omega \cdot cm^2$) = (cell pore resistance – blank hole resistance) × membrane area (4.67 cm^2).

After a period of time, the barrier layer formed, and a certain amount of ECM was added to both the upper and lower pools of the Transwell chamber to form a level difference of more than 0.5 cm. After 4 h, the liquid level difference was measured to confirm the barrier function of the cell layer.

Optical density (OD) of AChE

The OD of each component (AChE, nerve agent, and antidote) was tested and calculated before it was added to the modified Transwell system. AChE solutions with different concentrations were prepared using an ECM-phenol red free basic solution. The AChE activity was measured with the Ellman method, as previously described [21]. Samples were added to 96-well plates mixed with 8.6% acetylthiocholine (ATCh) and PBS and incubated at 37°C for 30 min. 5,5'-Dithiobis-(2-nitrobenzoic acid) (DTNB) was added to each well for the chromogenic reaction in the last step. ATCh would be degraded by the enzyme of AChE, and the degradation product can react with DTNB for chemiluminescence. The standard curve was calculated using the OD value from the sample plate, and the linear range of the enzyme solution was confirmed.

OD of the nerve agent sarin

AChE concentrations of 0.05, 0.06, and 0.07 mg/mL and sarin concentrations of 10^{-3}, 10^{-4}, 10^{-5}, 10^{-6}, and 10^{-7} v/v were used. AChE (1.6 mL) and sarin (0.4 mL) at each concentration was mixed successively in a six-well plate. After 3 min, samples were collected and detected by the Ellman method. The inhibition ratio was calculated using the following equation:

Inhibition rate of AChE (%) = (1 – inhibition group OD_{415nm}/non-inhibition group OD_{415nm}) × 100% [22].

Study of OD of reactivator

Four different reactivators (asoxime chloride [HI-6], obidoxime [LüH-6], pralidoxime chloride [2-PAM], and methoxime [MMB-4]), at concentrations of 0.05, 0.04, 0.03, 0.02, 0.01, and 0 mg/mL were mixed with AChE (0.07 mg/mL) and sarin (10^{-6} v/v). Ten minutes later, samples were collected and tested using the Ellman method. The reactivation rates of the reactivator at different concentrations were calculated using the following equation:

Reactivation rate (%) = (reactivator $group_{OD415nm}$ – inhibition group $_{OD415nm}$)/(normal $group_{OD415nm}$ – inhibition $group_{OD415nm}$) × 100% [13].

Therapeutic effect of the classical reactivator by modified Transwell model

AChE (0.07 mg/mL) and sarin (10^{-6} v/v) were simultaneously added to the lower chamber of the Transwell board, and then, the reactivators (0.03 mg/mL) were added to the upper chamber. After allowing time for the reactivator to penetrate the barrier and react with the inhibited enzyme, samples were collected from the lower chamber and detected by the Ellman method for enzyme activity, as previously described.

Preparation And Characterization Of The Liposomal Nanomedicine (LipoHI-6)

The proposed antidote (LipoHI-6) was prepared using an extrusion process [23]. Cholesterol (Chol) and DPPC mixed in a 2:1 molar ratio were dissolved and dispersed in chloroform and dried in a flask to produce a homogeneous lipid film by rotary evaporation. After adding to the HI-6 solution (2.2 mg/mL), ultrasonication was performed for 5 min to separate the film from the flask and encapsulate the HI-6 droplets to form a suspension. The suspension was then extruded successively 10 times through 200-nm and 100-nm polycarbonate filters using an Avanti Mini Extruder (Alabaster, AL, USA). Finally, the un-encapsulated free HI-6 was removed by dialysis with PBS. The size and zeta potential of LipoHI-6 were evaluated by dynamic light scattering (DLS) with a particle analyzer (Nano ZS90; Malvern Panalytical, Malvern, UK). The morphology of the LipoHI-6 nanoparticles was determined using TEM. The concentration of HI-6 loaded into the liposomes was quantified at 280 nm using a C_{18} column equipped with a UV detector in a high-performance liquid chromatography (HPLC) system (L7100; Hitachi, Tokyo, Japan) [18]. The mobile phase in the HPLC system comprised 15% acetonitrile and 85% H_2O at a flow rate of 2.0 mL/min. The encapsulation efficiency (EE%) and loading efficiency (LE%) of LipoHI-6 were evaluated using ultrafiltration/centrifugation. LipoHI-6 solution (1 mL) was sealed in a dialysis bag and suspended in 800 mL of PBS at pH 7.4 in a shaking incubator at 37°C to evaluate the release behavior of

the nanomedicine. Samples (1 mL) were collected for the system at a predetermined period and quantified by HPLC.

Permeability and therapeutic effect of LipoHI-6 according to the classical/modified Transwell model

The permeability of LipoHI-6 across the BBB was calculated using the classical Transwell model. LipoHI-6 (0.03 mg/mL) was added to the upper chamber, and 10 min later, samples collected from the lower chamber were quantified using HPLC. The permeability of HI-6 across the BBB was also tested using the same procedure as that for the control.

To evaluate the therapeutic effect of LipoHI-6, it was again added (0.03 mg/mL) to the upper chamber. At the same time, AChE was mixed with sarin in the lower chamber, as described previously. The activity of AChE after 10 min was analyzed using the Ellman method.

Animals

All experiments conformed to the Regulations of the Experimental Animal Administration issued by the State Committee of Science and Technology of the People's Republic of China (November 14, 1988). Sprague Dawley rats (2 weeks old; both specific pathogen-free) and Kunming (KM) mice (4 weeks old; both specific pathogen-free) were acquired from Beijing Charles River Laboratory Animal Technology Co, Ltd. (Beijing, China). Rodents had free access to sterilized food and distilled water and were maintained in stainless steel cages filled with hardwood chips in an air-conditioned room on a 12:12 h light/dark cycle.

Therapeutic effect of LipoHI-6 *in vivo*

The activity of central and peripheral AChE in KM mice was measured after sarin exposure and antidote administration. KM mice were randomly divided into four groups according to their body weight, with 12 mice in each group: normal group (no administration), poisoned group (only sarin poison), control group (poisoned and administered HI-6 [2.2 mg/mL]), and the liposomal nanomedicine group (poisoned and administered LipoHI-6 [2.2 mg/mL]). Mice were injected subcutaneously with sarin (180 μg/kg), followed by a subcutaneous antidote injection (10 μL/g) in the neck. The blood and brain were collected 10 min later, after which the brain tissue supernatant was obtained by centrifugation and diluted 500 times with PBS, and the activity of AChE in the sample was detected using the Ellman method.

Statistical analysis

Data are presented as means ± standard deviation (SD). An unpaired *t*-test was performed for two groups using GraphPad Prism 7.00 (GraphPad Software; San Diego, CA, USA). Statistical significance was set at $p < 0.05$.

Results

Growth and morphology of RBMECs

The morphological characterization of the RBMECs is shown in Fig. 1c. The RBMECs showed a bead-like appearance immediately after inoculation. After 16 h, the cells adhered to the wall and started growing. After 3 days of growth, the growth area of the endothelial cells started expanding continuously. After 8 days of culture, the cells were covered with a culture flask, and the shape of the paving-stone-like arrangement was observed. As shown by the RBMEC growth curve measured by CCK-8 (Fig. 1d), the logarithmic growth phase was observed on day 5, and peak growth occurred on days 7–8.

Evaluation of BBB model *in vitro*

After the RBMECs were incubated in T25 culture flasks for 6 days, tight junctions (TJs) were formed between cells, as observed by TEM (Fig. 1e). Throughout the 4-h leakage experiment, it was observed that the liquid level difference between the upper and lower pools of the Transwell plate could be maintained beyond 0.5 cm in the cell chambers (Fig. 1f). After 9 days of culture, the TEER reached 275 $\Omega \cdot cm^2$ (Fig. 1g).

Dosage of each component of the model

Different concentrations of AChE were detected by the Ellman method. The OD value obtained from Ellman method and the concentration of AChE showed good linearity in the range from 0.01 to 0.1 mg/mL, with a correlation coefficient (R^2) of 0.9946 (Fig. 1h). Furthermore, the inhibition rates (Fig. 1i) were investigated by the mixing of different concentrations of AChE (0.05–0.07 mg/mL) and sarin (10^{-3}–10^{-7} v/v). The maximum inhibition rates were in the order of 60%, 61% and 76% with AChE concentrations of 0.05, 0.06, and 0.07 mg/mL, respectively, and the inhibition rate increased with the amount of sarin. Detoxification effects of the four classical reactivators were evaluated to determine the amount of the reactivator used (Fig. 1j). The reactivation rates at 0.03 mg/mL AChE were 13%, 39%, 77%, and 53% for HI-6, LüH, 2-PAM, and MMB-4, respectively.

Therapeutic effect of the classical reactivator using the modified Transwell model

According to the modified Transwell model, the reactivation rates of HI-6, LüH, 2-PAM, and MMB-4 increased from 0.70–3.84%, 3.04–6.88%, 4.05–5.59%, and 3.33–5.85%, respectively, after reactivators were administered for 5 to 30 min (Fig. 1k).

Characterization of LipoHI-6 *in vitro*

TEM results showed that LipoHI-6 had a granular morphology and an obvious lipid bilayer structure at the nanoscale (Fig. 2a). The DLS results revealed that the average particle size was 147.8 ± 5.47 nm, with a polydispersity index (PDI) of 0.17 ± 0.03 (Fig. 2b). The charge of the liposome was close to neutral, and the average potential was 1.14 ± 1.31 mV (Table 1). The drug-releasing behaviors of LipoHI-6 and HI-6 solutions were measured using the rotating basket method. HI-6 was completely released within 40 min; in the same time, only about 25% of the HI-6 was released from LipoHI-6 (Fig. 2c). The entrapment and loading efficiencies of liposomes were 73.18% ± 3.26% and 18.92% ± 0.84%, respectively, as determined

by HPLC (Table 1). In the experiments on brain-target property, the amount of HI-6 delivered by the LipoHI-6 and HI-6 solutions and transported across the layer of the RBMECs into the lower chamber was determined by HPLC (Fig. 2d); within 10 min, the drug concentrations were 0.2 μg/mL and 0.6 μg/mL in the HI-6 and LipoHI-6 solutions, respectively, and there was a significant difference between the two concentrations ($p < 0.01$).

Therapeutic effect of LipoHI-6 *in vitro* and *in vivo*

The reactivation rates in the modified Transwell model are shown in Fig. 2e. The reactivation rate of the HI-6 group was only 6%, whereas that of the LipoHI-6 group was significantly different at 19% ($p < 0.001$). In further experiments on nerve agent detoxification in mice, the central reactivation rate of the animal model group treated with HI-6 was approximately 2%, and that of the group treated with LipoHI-6 was 20% (Fig. 2f). There was no significant difference between the reactivation rates of HI-6 and LipoHI-6, either in the traditional reactivation without the BBB *in vitro* (Fig. 2g) or the peripheral blood *in vivo* (Fig. 2h).

Table 1
Characterization of liposomes (mean ± SD; n = 4)

Drug loaded	Size (nm)	PDI	Zeta potential (mV)	EE%	LE%
HI-6	147.8 ± 5.47	0.17 ± 0.03	1.14 ± 1.31	73.18 ± 3.26	18.92 ± 0.84

Discussion

It is necessary to evaluate the drug detoxification effect in animal models in the final phase of research. The experimental procedure includes nerve agent poisoning, antidote administration, sample (brain and blood) collection, treatment (blood removal, dilution, and centrifugation), and measurement by the Ellman method, which requires a long time. Only one or two drugs could be evaluated in real time, because three animal groups (HI-6 treatment as the positive control, no antidote to determine the poison level, and no treatment or poisoning as the blank control) need to be considered and tested before drug evaluation. Moreover, ensuring the correct reactivation dates requires a refined nerve agent subcutaneous poisoning operation because small deviations in poison dosage and the direction and depth of insertion would cause a large error in the experimental results. In addition, nerve agent poisoning and antidote administration for each animal should be completed within 1 min of operation and repeated nearly 70 times. All these technical difficulties limit research into animal antidotes, especially with regard to the brain. Therefore, it is not appropriate to evaluate candidate drugs *in vivo* during the initial stage of drug screening, and *in vitro* drug evaluation might be more appropriate at this stage.

Based on these requirements, a modified simulated brain detoxification model integrating the Transwell system and reactivation evaluation required to be designed and constructed. In this model, the Transwell

board serves as a basic framework, and the RBMECs are planted in the middle membrane, forming a compact cell layer to simulate the BBB structure and achieve cell-level isolation. A reactivator was added to the upper chamber to simulate detoxification via intravenous administration. NAs and AChE were added and mixed in the lower chamber to simulate inhibition of AChE by NAs in the central nervous system (Fig. 1a). Only the drug molecules permeating the middle cell layer into the lower chamber could effectively combine with the nerve agent and peel it off from the enzyme to restore the activity. Finally, the therapeutic effect of drugs on sarin-inhibited AChE in the center could be directly determined by monitoring AChE activity in the lower chamber.

Original RBMECs were selected and extracted to build a barrier layer for the core of the system owing to the increased formation of dense TJs by the original cells compared to the subcultured ones (Fig. 1b). The cells showed a “paving stone” growth state 5 days after inoculation (Fig. 1c) and entered the logarithmic growth phase (Fig. 1d). During the logarithmic growth phase, stable and dense TJs (Fig. 1e) were formed between cells. The TEER of the Transwell system reached 275 $\Omega \cdot cm^2$ after cell inoculation on the membrane for 9 days (Fig. 1g), which indicated that the cells formed a stable and dense barrier layer on the membrane when the TEER exceeded 200 $\Omega \cdot cm^2$ [24, 25]. Furthermore, the compact barrier layer composed of RBMECs effectively prevented the liquid from penetrating the upper chamber, as demonstrated by the stable liquid level difference in the 4-h leakage experiment (Fig. 1f).

In the next stage, each component in the Ellman method was integrated into the Transwell system, which met two basic requirements: maintaining the activity of the AChE chromogenic reaction and avoiding damage to the cell barrier layer. Therefore, the use of each component was monitored and evaluated to ensure the minimum effective dosage and protection of cells. First, the concentration of AChE chosen for integration in the Ellman method must be within the linear concentration range to ensure accuracy of the AChE chromogenic reaction. However, at an AChE concentration as low as 0.07 mg/mL, the inhibition rate was lower than 75% regardless of the amount of sarin used (Fig. 1i). One prerequisite for reactivator evaluation was that the modified model be in a severely acute poisoning state, implying that the inhibition rate be higher than 70% [26]. Therefore, the lowest dose of AChE was determined to be 0.07 mg/mL. Second, to reduce stimulation and ensure the integrity of the endothelial vascular layer, the lowest dose of sarin (10^{-6} v/v) was chosen when the inhibition rate reached 75% (Fig. 1i). Third, the antidote effectively counteracted the nerve agent when the reactivation rate of central AChE reached 10%, as shown in previous reports [27]; therefore, drugs with a reactivation rate of more than 10% *in vitro* were added to the upper pool. The reactivation rates of the four classic reactivators at different concentrations (Fig. 1j) could exceed 10% when the concentration was higher than 0.03 mg/mL, which was selected as the screening drug concentration for preferential consideration. Thus, the appropriate concentration and dosage of each component (enzymes, NAs, and candidate drugs) were determined individually to satisfy the requirements.

The four classic reactivators were further evaluated using modified Transwell and normal models. Without the cell barrier layer, all drugs could effectively attach to the inhibited enzyme to achieve good treatment effect (up to 72% [the minimum HI-6 was only 26%]) (Table 2). With the cell barrier, the

reactivation rate of all drugs reached only 5.09%. The reactivation rate of all drugs gradually increased (Fig. 1k) but did not reach 10% throughout administration, while HI-6 displayed the lowest therapeutic effect among the four reactivators. The results revealed that most of the hydrophilic reactivators were blocked by the barrier cell layer to counteract the NAs; only very small amounts of reactivators permeated the layer, and the amount only increased slightly with extended periods of administration. It has been proven that extremely serious errors would occur in the absence of a simulated barrier layer in drug evaluation models [14]; drug screening in a reaction model without a barrier layer cannot really reflect the effect of drug treatments.

Table 2
Reactivation rate of acetylcholinesterase (AChE) using four classic reactivators

Reactivator	Reactivation rate of AChE (%)	
	Model group	Control group
HI-6	0.74 ± 0.94***	26.85 ± 9.15
LuH	5.09 ± 0.41***	55.78 ± 5.88
2-PAM	4.73 ± 1.69***	72.17 ± 4.75
MMB-4	3.96 ± 1.01***	63.54 ± 10.58
Mean ± SD; n = 4; ***$p < 0.001$ compared to the control group		

In addition to evaluating small-molecule drugs, the modified Transwell model was used to evaluate the reactivation rate of the nanomedicine. The treatment effect of the nanomedicine *in vivo* was also processed at the same time to verify the effectiveness of the modified Transwell model. Liposomes with sizes < 200 nm (Fig. 2a) were successfully synthesized by using the classic blown film extrusion method, which consisted of a shell of DPPC and Chol and a core of HI-6 solution. Owing to the advantage of the high lipolytic action of the liposome shell, the nanoparticles are able to permeate the BBB [28–30]. The DLS results showed that the particle size distribution of the synthesized liposomes was uniform (Fig. 2b). Compared to the profile of the HI-6 solution, HI-6 was released more slowly from the liposomes (Fig. 2c). In the classical Transwell system, HI-6 carried by the nanoparticles effectively penetrated the cell barrier layer of the Transwell system into the lower chamber, as quantified by HPLC. The drug concentration in the liposome group was more than three times higher than that in the HI-6 group (Fig. 2d), indicating that the synthesized liposome nanoparticles had a certain central targeting ability.

Further evaluation using the modified Transwell model showed that the reactivation rate of the LipoHI-6 group was 19%, and that of the HI-6 group was 6% (Fig. 2e), which proved that the liposomal nanoparticles could more effectively permeate the cell barrier layer of the Transwell system and successfully reactivate sarin-inhibited AChE. Meanwhile, in the reactivation experiments using the animal poisoning model (Fig. 2f), the central reactivation rate of LipoHI-6 was significantly higher than that of

the HI-6 solution. In the peripheral environment of blood circulation, which has no physiological barrier, the reactivation rates of LipoHI-6 and HI-6 showed no significant difference (Fig. 2h), which was similar to the results in the traditional *in vitro* model without the cell barrier layer representing the BBB (Fig. 2g). However, all of the data accessed from the *in vitro* and *in vivo* models led to the same conclusion, which means that the modified *in vitro* model could realistically reflect the drug treatment effect.

Therefore, the three models were comprehensively compared (Table 3). We found that the traditional model *in vitro* (without a cell layer) had the advantages of simplicity, low time requirement, and low dosages of toxic agents; however, it can only reflect the interaction between drugs and poisons without characterization of the central targeting ability. The result obtained from the animal poisoning model was closest to the true fact. However, the complex operation and requirement of more manpower and higher dosages of NAs limit the application of the method. The modified model detailed in this study combines the advantages of the two previously described models and can achieve rapid, accurate, and large-scale drug screening.

Table 3
Comparison of requirements among different exposure models

Evaluation index	**Evaluation method**		
	Animal model	***In vitro* central exposure model**	**Single-reaction environment model**
Assessable drug quantity	2	6	6
Quantity of animals required	100	12	None
Accuracy of results	The individual difference is obvious, and the results are realistic	The individual difference is not obvious, and the results are somewhat realistic	Data are uniform, and the results are not close to the reality
Time required for evaluation	2 (h)	5 (h)	0.5 (h)
Number of personnel required	5 (person)	1 (person)	1 (person)
Required amount of poison	10^{-5} v/v × 20 mL	10^{-6} v/v × 10 mL	10^{-6} v/v × 10 mL
Multiple replicates of the same sample	No	Yes	No

Conclusion

In this study, a modified *in vitro* model for nerve agent reactivation was successfully established. Our results show that this modified model can simulate the situation of central poisoning with a physiological barrier representing the BBB, effectively avoid individual differences and other factors, and accurately reflect the central drug treatment effects. Moreover, the central poisoning AChE can be monitored in real time. In addition, at least six candidate drugs can be screened in one experiment, which is convenient for large-scale drug screening. Therefore, the modified model can simultaneously investigate the central targeting and reactivation ability of drugs and effectively promote the research and development of centrally applied drugs.

Furthermore, a new brain-targeting nanomedicine was synthesized, and this modified model was evaluated. The results obtained from the modified model showed that the nanomedicine allowed for central targeting and effectively reactivated the central AChE, which was consistent with the data obtained from the animal poisoning model. All results show that the modified model is suitable for the evaluation of nanomedicine in addition to small molecules, and the nano-delivery system had good prospects for the application of brain disease treatments.

Abbreviations

ACh: Acetylcholine

AChE: Acetylcholinesterase

ATCh: Acetylthiocholine

BBB: Blood–brain barrier

CCK-8: Cell Counting Kit-8; Chol: Cholesterol

DLS: Dynamic light scattering

DTNB: 5,5'-Dithiobis-(2-nitrobenzoic acid)

DPPC: Dipalmitoylphosphatidylcholine

ECM: Endothelial cell medium

HI-6: Asoxime chloride

HPLC: High-Performance Liquid Chromatography

LuH: Obidoxime

MMB-4: Methoxime

NAs: Nerve agents

PBS: Phosphate-buffered saline

PDI: Polydispersity index

RBMECs: Rat brain microvascular endothelial cells

SD: Standard deviation

TEER: Transendothelial electrical resistance

TEM: Transmission electron microscope

TJ: Tight junction

2-PAM: Pralidoxime chloride

Declarations

Acknowledgments

We would like to express our gratitude to all laboratory members for their assistance.

Authors' contributions

Yao Li, Jun Yang, and Yongan Wang conceived and designed the study. Yao Li, Jingyi Huang, Huanchun Xing, Zinan Zhang, and Xin Sui conducted the experiments. Yuan Luo analyzed the data. Jun Yang and Yongan Wang supervised the study and edited the manuscript. All authors read and approved the manuscript.

Funding

This work was supported by the Beijing Science and Technology New Star Project (Z191100001119105), the National Defense Science and Technology Innovation Project (1716312ZT00114601), and the Innovation Project of General Logistics Department (16CXZ031).

Availability of data and materials

The datasets generated and/or analyzed during the current study are available from the corresponding author upon reasonable request.

Ethics approval and consent to participate

All experiments conformed to the Regulations of the Experimental Animal Administration issued by the State Committee of Science and Technology of the People's Republic of China (November 14, 1988).

Consent for publication

Not applicable.

Competing interests

The authors declare that they have no competing interests.

References

1. Weir AGA, Makin S, Breeze J. Nerve agents: emergency preparedness. BMJ Mil Health. 2020;166(1):42-6.
2. Worek F, Szinicz L, Eyer P, Thiermann H. Evaluation of oxime efficacy in nerve agent poisoning: development of a kinetic-based dynamic model. development of a kinetic-based dynamic model. Toxicol Appl Pharmacol. 2005;209(3):193-202.
3. Haines DD, Fox SC. Acute and long-term impact of chemical weapons: lessons from the Iran-Iraq war. Forensic Sci Rev. 2014;26(2):97-114.
4. Aroniadou-Anderjaska V, Apland JP, Figueiredo TH, Furtado MDA, Braga MF. Acetylcholinesterase inhibitors (nerve agents) as weapons of mass destruction: History, mechanisms of action, and medical countermeasures. Neuropharmacology. 2020:108298.
5. Rosman Y, Eisenkraft A, Milk N, Shiyovich A, Ophir N, Shrot S, et al. Lessons learned from the Syrian sarin attack: evaluation of a clinical syndrome through social media. Ann Intern Med. 2014;160(9):644-8.
6. Tokuda Y, Kikuchi M, Takahashi O, Stein GH. Prehospital management of sarin nerve gas terrorism in urban settings: 10 years of progress after the Tokyo subway sarin attack. Resuscitation. 2006;68(2):193-202.
7. Vale JA, Marrs TC, Maynard RL. Novichok: a murderous nerve agent attack in the UK. Clin Toxicol. 2018;56(11):1093-7.
8. Hulse EJ, Haslam JD, Emmett SR, Woolley T. Organophosphorus nerve agent poisoning: managing the poisoned patient. Br J Anaesth. 2019;123(4):457-63.
9. Sakurada K, Ohta H. No promising antidote 25 years after the Tokyo subway sarin attack: a review. Leg Med. 2020;101761.
10. Santoni G, de Sousa J, de la Mora E, Dias J, Jean L, Sussman JL, et al. Structure-based optimization of nonquaternary reactivators of acetylcholinesterase inhibited by organophosphorus nerve agents. J Med Chem. 2018;61(17):7630-9.
11. Kalász H, Nurulain S, Veress G, Antus S, Darvas F, Adeghate E, et al. Mini review on blood–brain barrier penetration of pyridinium aldoximes. J App Toxicol. 2015;35(2):116-23.
12. Dadparvar M, Wagner S, Wien S, Kufleitner J, Worek F, von Briesen H, et al. HI 6 human serum albumin nanoparticles—Development and transport over an in vitro blood–brain barrier model.

Toxicol Lett. 2011;206(1):60-6.

13. Yang J, Fan L, Wang F, Luo Y, Sui X, Li W, et al. Rapid-releasing of HI-6 via brain-targeted mesoporous silica nanoparticles for nerve agent detoxification. Nanoscale. 2016;8(18):9537-47.
14. Wagner S, Kufleitner J, Zensi A, Dadparvar M, Wien S, Bungert J, et al. Nanoparticulate transport of oximes over an in vitro blood-brain barrier model. PloS One. 2010;5(12):e14213.
15. Cardoso FL, Brites D, Brito MA. Looking at the blood–brain barrier: molecular anatomy and possible investigation approaches. Brain Res Rev. 2010;64(2):328-63.
16. Perrière N, Yousif S, Cazaubon S, Chaverot N, Bourasset F, Cisternino S, et al. A functional in vitro model of rat blood–brain barrier for molecular analysis of efflux transporters. Brain Res. 2007;1150:1-13.
17. Coisne C, Dehouck L, Faveeuw C, Delplace Y, Miller F, Landry C, et al. Mouse syngenic in vitro blood–brain barrier model: a new tool to examine inflammatory events in cerebral endothelium. Lab Investig. 2005;85(6):734-46.
18. Zhang Y, He J, Shen L, Wang T, Yang J, Li Y, et al. Brain-targeted delivery of obidoxime, using aptamer-modified liposomes, for detoxification of organophosphorus compounds. J Control Release. 2020.
19. Perriere N, Demeuse P, Garcia E, Regina A, Debray M, Andreux JP, et al. Puromycin-based purification of rat brain capillary endothelial cell cultures. Effect on the expression of blood–brain barrier-specific properties. J Neurochem. 2005;93(2):279-89.
20. Shayan G, Choi YS, Shusta EV, Shuler ML, Lee KH. Murine in vitro model of the blood–brain barrier for evaluating drug transport. Eur J Pharm Sci. 2011;42(1-2):148-55.
21. Ellman GL, Courtney KD, Andres Jr V, Featherstone RM. A new and rapid colorimetric determination of acetylcholinesterase activity. Biochem Pharmacol. 1961;7(2):88-95.
22. Järvinen P, Vuorela P, Hatakka A, Fallarero A. Potency determinations of acetylcholinesterase inhibitors using Ellman's reaction-based assay in screening: Effect of assay variants. Anal Biochem 2011;408(1):166-8.
23. Lin C-Y, Li R-J, Huang C-Y, Wei K-C, Chen P-Y. Controlled release of liposome-encapsulated temozolomide for brain tumour treatment by convection-enhanced delivery. J Drug Target. 2018;26(4):325-32.
24. Abbott NJ, Dolman DE, Drndarski S, Fredriksson SM. An improved in vitro blood–brain barrier model: rat brain endothelial cells co-cultured with astrocytes. astrocytes. Methods Mol Biol. 2012; 814:415-30.
25. Hemmelmann M, Metz VV, Koynov K, Blank K, Postina R, Zentel R. Amphiphilic HPMA–LMA copolymers increase the transport of Rhodamine 123 across a BBB model without harming its barrier integrity. J Control Release. 2012;163(2):170-7.
26. Chambers JE, Carr RL. Inhibition patterns of brain acetylcholinesterase and hepatic and plasma aliesterases following exposures to three phosphorothionate insecticides and their oxons in rats. Toxicol Sci. 1993;21(1):111-9.

27. Bajgar J, Fusek J, Kassa J, Jun D, Kuca K, Hajek P. An attempt to assess functionally minimal acetylcholinesterase activity necessary for survival of rats intoxicated with nerve agents. Chem-Biol Interact. 2008;175(1-3):281-5.
28. Agrawal M, Saraf S, Saraf S, Dubey SK, Puri A, Patel RJ, et al. Recent strategies and advances in the fabrication of nano lipid carriers and their application towards brain targeting. J Control Release 2020;321:372-415.
29. Fowler M, Cotter J, Knight B, Sevick-Muraca E, Sandberg D, Sirianni R. Intrathecal drug delivery in the era of nanomedicine. Adv Drug Deliv Rev. 2020;165:77-95.
30. Pastorino F, Brignole C, Di Paolo D, Perri P, Curnis F, Corti A, et al. Overcoming biological barriers in neuroblastoma therapy: the vascular targeting approach with liposomal drug nanocarriers. Small. 2019;15(10):1804591.

Figures

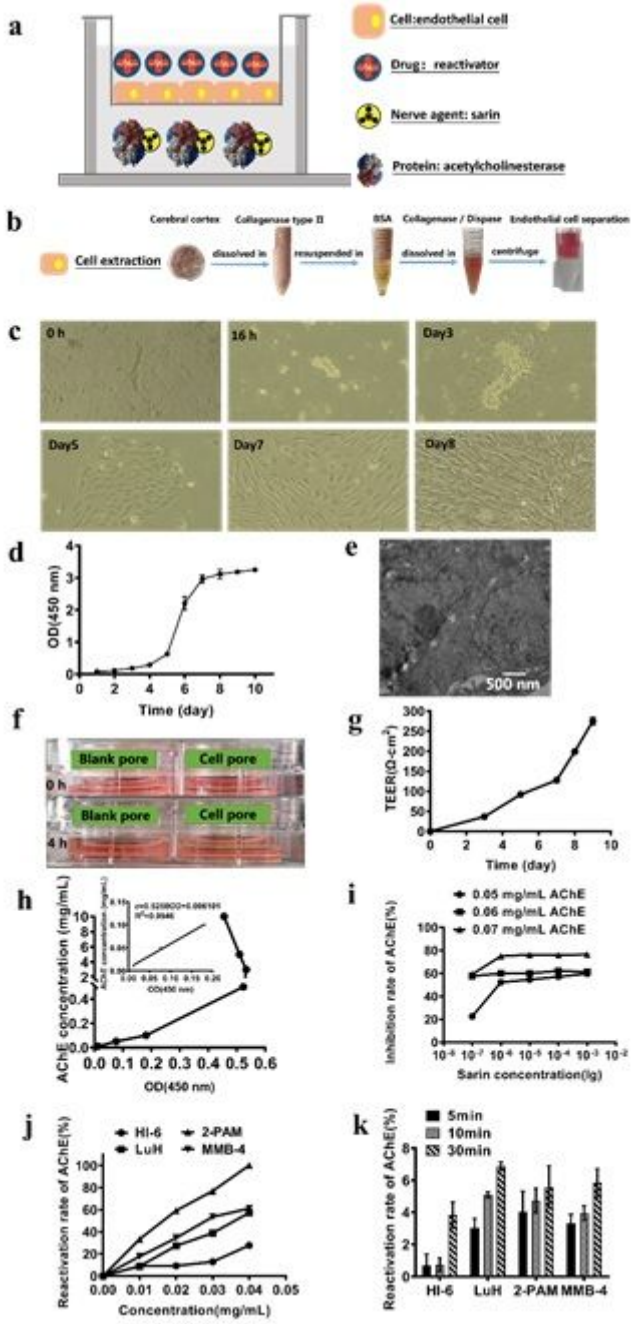

Figure 1

Schematic representation and characterization of the in vitro nerve agent brain poisoning Transwell model. a. Components of the Transwell model. b. Rat brain microvascular endothelial cell (RBMEC) extraction process. c. Growth process and morphological changes in rat brain microvascular endothelial cells (RBMECs). d. RBMEC growth curve (n = 6). e. Transmission electron microscopy (TEM) photographs of the tight junction (TJ). The scale bar indicates 500 nm. f. Experimental results of leakage at 4 h. g. Correlation of transendothelial electrical resistance (TEER) assay with RBMEC culture time (n = 4). h. Determination of the standard curve of acetylcholinesterase (AChE) using the Ellman method. i, j. The dosage of AChE, sarin, and reactivator for the in vitro nerve agent poisoning Transwell model was determined. k. Evaluation of the model with reactivating agents commonly used in clinic (n = 4).

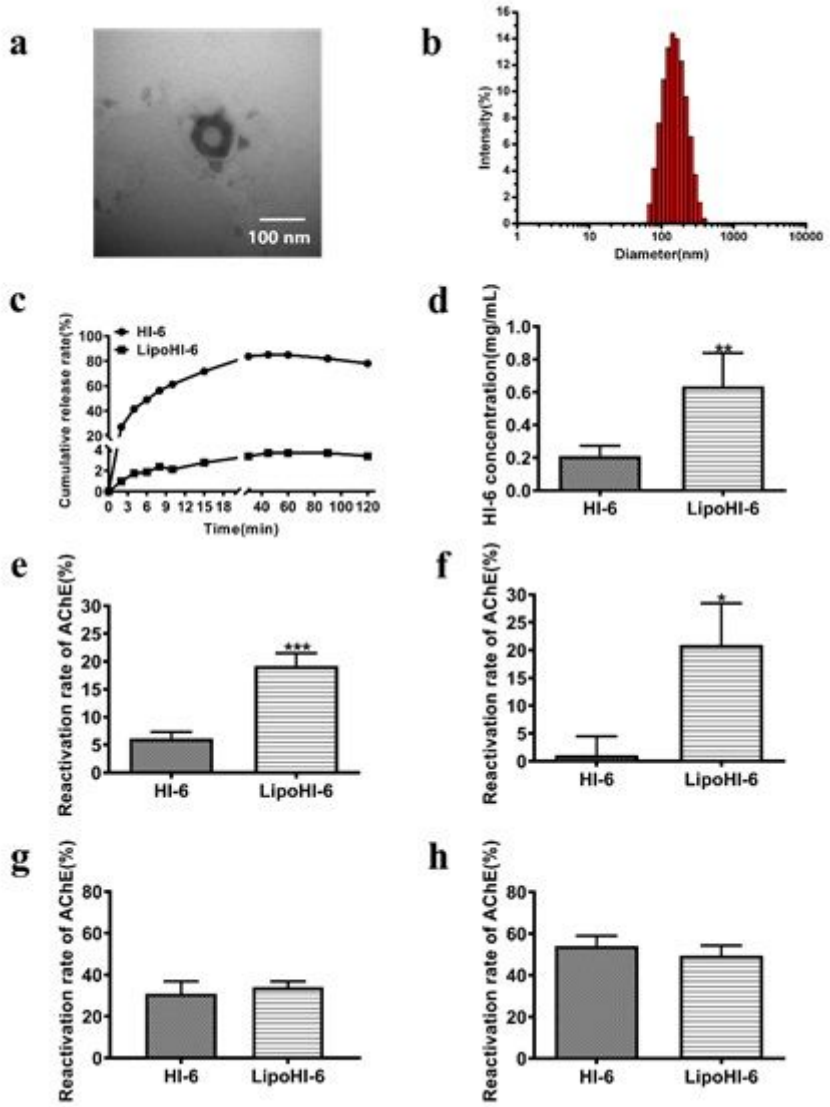

Figure 2

Characterization of LipoHI-6 and its therapeutic effect in vitro and in vivo. a. Transmission electron microscopy (TEM) photographs of LipoHI-6. The scale bar indicates 100 nm. b. Size of LipoHI-6. c. Release kinetics of HI-6 and LipoHI-6 under simulated physiological conditions at pH 7.4. d. Permeability of the blood–brain barrier for LipoHI-6 (mean ± SD; n = 4), **p < 0.01 compared to HI-6. e. Evaluation of the therapeutic effect of LipoHI-6 on sarin-inhibited enzyme in the in vitro nerve agent poisoning Transwell model (mean ± SD; n = 5), ***p < 0.001 compared to HI-6. f. Central reactivation rate of LipoHI-6 in an animal model (mean ± SD; n = 12), *p < 0.05 compared to HI-6. g. Evaluation of the therapeutic effect of LipoHI-6 on the sarin-inhibited enzyme in vitro (mean ± SD; n = 5). h. Peripheral reactivation rate of LipoHI-6 in an animal model (mean ± SD; n = 12).